



## **Multi-tonal low frequency noise control for aircraft cabin using Helmholtz resonator with complex cavity**

Tenon Charly Kone<sup>1</sup>

National Research Council Canada, Flight Research Laboratory  
1200 Montreal Road, Ottawa, ON, K1A 0R6, Canada.

Sebastian Ghinet<sup>2</sup>

National Research Council Canada, Flight Research Laboratory  
1200 Montreal Road, Ottawa, ON, K1A 0R6, Canada.

Raymond Panneton<sup>3</sup>

Department of Mechanical Engineering, Université de Sherbrooke, Groupe d'Acoustique de l'Université de Sherbrooke (GAUS)  
2500 Boulevard de l'Université, Sherbrooke, QC, J1K 2R1, Canada.

Thomas Dupont<sup>4</sup>

Department of Mechanical Engineering, École de Technologie Supérieure,  
1100, rue Notre-Dame Ouest, Montréal, QC, H3C 1K3, Canada

Anant Grewal<sup>5</sup>

National Research Council Canada, Flight Research Laboratory  
1200 Montreal Road, Ottawa, ON, K1A 0R6, Canada.

### **ABSTRACT**

**The noise control at multiple tonal frequencies simultaneously, in the low frequency range, is a challenge for aerospace, ground transportation and building industries. In the past few decades, various low frequency noise control solutions, based on acoustic metamaterials designs, have been presented in the literature. The proposed technologies showed promising acoustic performances and are considered as better solutions when compared to conventional sound insulation materials. Previously, presented approaches combining layered porous materials with embedded Helmholtz resonators have shown interesting potential when tuned at multi-tonal frequencies. In the extension of these previous works, this article proposes a metamaterial**

---

<sup>1</sup> [TenonCharly.Kone@nrc-cnrc.gc.ca](mailto:TenonCharly.Kone@nrc-cnrc.gc.ca)

<sup>2</sup> [Sebastian.Ghinet@nrc-cnrc.gc.ca](mailto:Sebastian.Ghinet@nrc-cnrc.gc.ca)

<sup>3</sup> [Raymond.Panneton@nrc-cnrc.gc.ca](mailto:Raymond.Panneton@nrc-cnrc.gc.ca)

<sup>4</sup> [Thomas.Dupont@etsmtl.ca](mailto:Thomas.Dupont@etsmtl.ca)

<sup>5</sup> [Anant.Grewal@nrc-cnrc.gc.ca](mailto:Anant.Grewal@nrc-cnrc.gc.ca)

consisting of a structured Helmholtz (HR) resonator integrated in a glass wool matrix to improve sound transmission loss (STL), and simultaneously control noise at several tonal frequencies. The HR is a cylindrical cavity with an internal structured neck. The structured neck consists of a main cylindrical pore supporting periodic cavities along its axis. The analytical modeling of the proposed metamaterial uses the transfer matrix method (TMM) in series and in parallel. The present investigation shows that this type of metamaterial makes it possible to control multitone noise and to shift transmission loss peaks towards low frequencies. It was observed that the STL calculated using the developed TMM approach was in good agreement with that resulting from a modeling by the finite element method (FEM).

## 1. INTRODUCTION

Along with all the technological, operational and regulatory barriers, Unmanned Aerial System (UAS) Noise generation has been identified as a significant factor limiting the widespread adoption of UAS systems, particularly within densely populated regions. Understanding and mitigating the acoustic emissions from UAS systems poses a significant challenge due to their unconventional vehicle layout with multiple propulsions units combined with their operation in reverberant urban environments at high thrust levels.

One of the main sources of noise from Unmanned Aerial System (UAS) is tonal noise. This noise comprises noise components of the interaction of the rotors with the stators (the fixed walls like the shoulder supports), known as the blade passing noise and the engine noise [1-3]. Several methods of tonal noise reduction are available in the literature. Noise attenuation can be achieved at the source by proper design of the propeller blades and / or support (Stator) [4-6]. This approach requires very advanced knowledge in the design of turbomachines and is often very expensive in terms of computation time and numerical implementation effort. Another approach which is increasingly being used is that of reduction during the propagation of noise in space. A common practice for early aircraft engines is to shroud the rotors within a duct lined with an acoustic treatment or acoustic liner. The latter practice has the advantage of improving both aerodynamic [7, 8] and aeroacoustics performance [9-11]. Acoustic liner could be very effective in reducing the tonal noise generated by the propeller and engine. But the conventional acoustic liner requires additional weight and installation space which represents a critical challenge to attain on the UAS platform. One of the promising paths is the coupling between conventional porous absorbers or membrane and resonators (acoustic metamaterials). The research on acoustic insulation metamaterials is relatively recent. Beck *et al.* [12, 13] have designed an acoustic metamaterial with an array of Helmholtz resonators separated by quarter-wave volumes. The results indicated that normal incidence absorption coefficient of this liner was more than 10 times larger compared with conventional honeycomb liner at the designed Helmholtz resonance frequency. Auregan *et al.* [14, 15] presented a thin sub-wavelength metamaterial embedded in an airflow channel. The material used was made of a series of thin rectangular tubes mounted in parallel on the inner surface of the airflow channel. They showed that this optimized material gives a significant attenuation at low frequencies. This material has proven to be a possible solution for airflow channels when space constraints and low frequency noise render quarter wave resonators unusable. García-Chocano *et al.* [16] demonstrated a large reduction in the transmitted waves in a duct using a quarter-wave resonator metamaterial, which was similar to a traditional perforate over honeycomb core liner. Therefore, these literature reviews have shown that it should be possible to incorporate these metamaterial structures into an acoustic coating to increase the low frequency performance of UAS ducting.

Recently, an additional form of innovative, thin acoustic metamaterials capable of absorbing multiple frequencies at the same time such as multiple blade pass frequencies was proposed. These new concepts of thin geometry were first proposed by Leclaire *et al.* [17], then improved by Dupont *et al.*

[18-20]. The proposed design comprised a perforated material for which the main perforations were connected to an array of periodically spaced very thin annular dead-end pores with respect to the lateral size. This solution consisted in connecting dead-end pores, i.e., thin cavity resonators, on a main tubular pore to create dead-end porosity materials. One of the advantages of this metamaterial design was to shift the resonance frequencies of the metamaterial (absorption peaks) towards the low-frequencies. This can be explained by an increase in the effective compressibility of the material. Although these studies have shown growing potential of thin metamaterials, they have never been used in UAS ducts. In addition, the coupling of these metamaterials with conventional sound absorbing materials, such as glass wool, have not yet been investigated.

The objective of this paper is to develop a metamaterial which can be integrated into a duct and capable of attenuating the noise at several UAS blade passage frequencies. Moreover, the present paper proposes a fast and reliable methodology for the characterization of the acoustic properties of the metamaterial. The proposed thin metamaterial is a Helmholtz resonator (HR) embedded in a glass wool matrix. The neck of the HR is structured as the metamaterial described in Kone *et al.* [19, 20]. Serial and parallel transfer matrix methods (TMM and PTMM) [21, 22] are used to construct the transfer matrix of the metamaterial and to predict its normal incidence sound absorption coefficient and transmission loss.

## 2. MATERIALS

The objective of this study is to develop and characterize the acoustic performance of a metamaterial capable of attenuating noise at several blade passage frequencies of an ASU rotor ducted at low frequencies. The metamaterial under study consists of a circular cylindrical Helmholtz (HR) resonator embedded in a glass wool matrix. The HR has an internal circular cylindrical structured neck comprising a periodic alternation of sub-necks and cavities. Figure 1 shows the geometric details of the metamaterial (note that the geometry is axisymmetric). As it can be seen, the resonator is divided into three parts. Parts A and B are filled with air at rest, where thermo-viscous losses are neglected due to the large volume-to-surface ratios. Part C is the structured neck of the HR made of  $N$  successions of the periodic cell shown in Figure 1 (b). The structured neck is saturated with air at rest. Upstream and downstream of the structured neck, an extra thickness of half a sub-neck is added so that each annular cavity wall is of thickness  $l$ . Since the volume-to-surface ratios in the structured neck are small, thermo-viscous losses will have to be considered in the calculation of the effective air properties in the sub-necks and in the cavities.

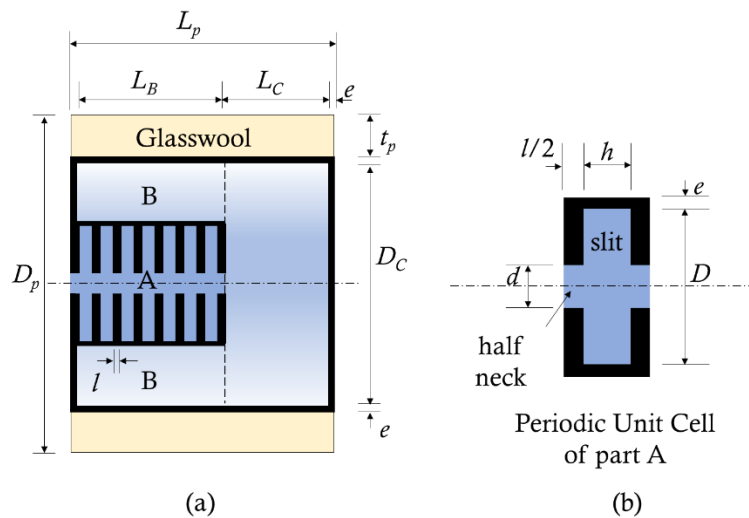


Figure 1: Metamaterial under study. (a) Helmholtz resonator, with a structured neck, embedded in glass wool. (b) Zoom on the structured neck of the Helmholtz resonator.

### 3. MODELING OF THE METAMATERIAL

In order to quickly characterize the acoustic performance of the metamaterial, the transfer matrix method (TMM) has been adopted. In what follows, the transfer matrix (TM) of each part of the metamaterial is presented as well as the assembly method making it possible to construct the global transfer matrix of the metamaterial. This global transfer matrix will make it possible to calculate the sound absorption coefficient (on a rigid wall) and the sound transmission loss of the metamaterial.

#### 3.1. Helmholtz resonator

The HR is the superposition of parts A, B and C shown in Figure 1. To build its TM, it is necessary to develop the TM of each of its three parts.

- **Part A (structured neck)**

Part A is the structured neck of the HR. It is similar to the metamaterial studied by Kone *et al.* [19, 20]. In order to calculate its transfer matrix, surface impedance relations on its periodic unit cell (PUC) will be developed. The PUC is axisymmetric. It is defined as an assembly of two cylindrical half-necks, a central cylindrical volume, and an annular cylindrical cavity. In Figure 2, the central volume is denoted V, and the annular cavity is denoted slit. We have chosen to designate the cavity by the word "slit" to emphasize the fact that the width  $h$  of the cavity is narrow and that it could be modeled as a slit to take account of thermo-viscous losses.

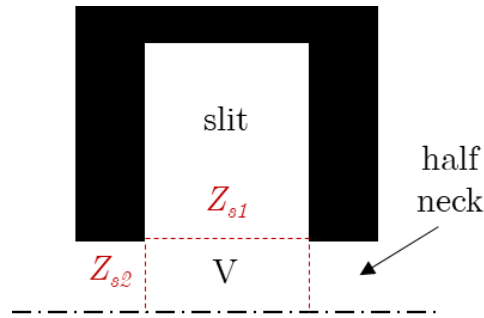


Figure 2: PUC of the axisymmetric structured neck with locations of surface impedances.

In accordance with the lumped model proposed by Dupont *et al.* [18], which is based on the surface impedance of the cavity given by Dickey et Selamet [24], the acoustic surface impedance  $Z_{s_1}$  at the junction of the central volume V and the annular slit is given by the following relation

$$Z_{s_1} = jZ_{slit} \frac{H_0^1(k_{slit} d/2) - H_0^2(k_{slit} d/2) H_1^1(k_{slit} D/2)/H_1^2(k_{slit} D/2)}{H_1^1(k_{slit} d/2) - H_1^2(k_{slit} d/2) H_1^1(k_{slit} D/2)/H_1^2(k_{slit} D/2)} \quad (1)$$

where  $H_v^m$  is the Hankel function of  $v$ -th order and  $m$ -th kind,  $k_{slit}$  and  $Z_{slit}$  are the effective complex wave number and characteristic impedance of the air in the slit. These effective properties consider the thermo-viscous losses using the Johnson-Champoux-Allard (JCA) model [23] with the corresponding slit parameters given in Table 1.

The acoustic surface impedance  $Z_{s_2}$  at the interface between the half-neck and the slit can be deduced using Equation 24 of Reference [24] and is given by

$$Z_{s_2} = \frac{1}{\frac{1}{hjk/Z_0} + 4/Z_{s_1}d} \quad (2)$$

where  $k$  and  $Z_0$  are the wavenumber and the characteristic impedance of the air at rest. Here, these properties are real since the central volume does not include walls on which thermo-viscous losses would occur. Knowing the surface impedance of the slit, its transfer matrix is given

$$T_{\text{slit}} = \begin{pmatrix} 1 & 0 \\ 1/Z_{s_2} & 1 \end{pmatrix}. \quad (3)$$

The transfer matrix  $T_{1/2}$  of each half-neck on either side of the slit is given by:

$$T_{1/2} = \begin{pmatrix} \cos(k_{1/2} l'/2) & jZ_{1/2}\sin(k_{1/2} l'/2) \\ \frac{j}{Z_{1/2}}\sin(k_{1/2} l'/2) & \cos(k_{1/2} l'/2) \end{pmatrix} \quad (4)$$

where  $k_{1/2}$  and  $Z_{1/2}$  are the effective complex wavenumber and characteristic impedance of the air in the neck which consider for thermo-viscous losses. They were calculated using the JCA model [23] and the corresponding circular neck parameters given in Table 1. In Equation 4,  $l' = l + 0.85d/2$  is the effective length to account for end correction.

With the previous transfer matrix, the transfer matrix of the PUC is defined as:

$$T_{\text{PUC}} = T_{1/2}T_{\text{slit}}T_{1/2}. \quad (5)$$

Since  $N$  PUCs are assembled together, the transfer matrix of this assembly is given by raising the matrix of Equation 5 to the power of  $N$ . Also, to complete the construction of the transfer matrix of the structured neck described in Figure 1, one half-neck has to be added on both ends of the PUC. Then, the transfer matrix of the structured neck becomes:

$$T_A = T_{1/2}(T_{\text{PUC}})^N T_{1/2}. \quad (6)$$

Table 1: Johnson-Champoux-Allard (JCA) [23] parameters of the slit and half-neck, where  $\eta$  is the dynamic viscosity of air.

| Pore type | Viscous and thermal characteristic lengths<br>$\Lambda$ (mm) | Tortuosity<br>( $\alpha_\infty$ ) | Static airflow resistivity<br>$\sigma$ ( $\text{Pa}\cdot\text{s}/\text{m}^2$ ) | Open porosity<br>$\Phi$ (%) |
|-----------|--|-----------------------------------|--|-----------------------------|
| Slit      | $h$  | 1                                 | $12\eta/h^2\Phi$   | 100                         |
| Circular  | $d/2$  | 1                                 | $32\eta/d^2\Phi$   | 100                         |

- **Parts B and C (hard walled cavities of the HR)**

In accordance with the modeling of axisymmetric reactive silencers comprising an inlet expansion chamber [25], parts B and C are seen as two parallel branches in contact with the sub-neck of part A. The equivalent admittance model of this configuration is shown in Figure 3. As the walls of parts B and C are acoustically rigid, the surface admittances of parts B and C at the junction with the sub-neck of part A are respectively given by:

$$Y_B = \frac{S_B}{S_d Z_0} \tanh(jkL_B)$$

$$Y_C = \frac{S_C}{S_d Z_0} \tanh(jkL_C)$$
(7)

where  $S_B$  and  $S_C$  are the cross-section areas of parts B and C, respectively, and  $S_d$  is the cross-section area of the sub-neck. Consequently, the transfer matrix of parts B and C in parallel is given by

$$\mathbf{T}_{BC} = \begin{pmatrix} 1 & 0 \\ Y_B + Y_C & 1 \end{pmatrix}$$
(8)

Combining in series transfer matrices  $\mathbf{T}_A$  and  $\mathbf{T}_{BC}$  yields the transfer matrix of the Helmholtz resonator. It is given by:

$$\mathbf{T}_{HR} = \mathbf{T}_A \mathbf{T}_{BC}$$
(9)

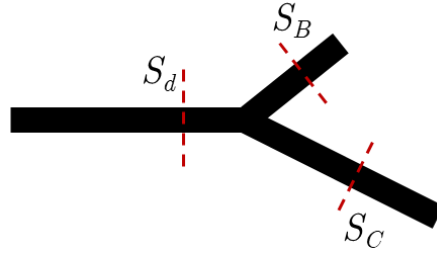


Figure 3: Admittance model of the Helmholtz resonator with its internal structured neck and air cavity volumes.

### 3.2. Glass wool

The transfer matrix of the glass wool is directly derived from the JCA equivalent fluid model [23]. This transfer matrix is given by

$$\mathbf{T}_{GW} = \begin{pmatrix} \cos(k_{gw}L_p) & jZ_{gw}\sin(k_{gw}L_p) \\ \frac{j}{Z_{gw}}\sin(k_{gw}L_p) & \cos(k_{gw}L_p) \end{pmatrix}$$
(10)

where  $k_{gw}$  and  $Z_{gw}$  are the effective complex wavenumber and characteristic impedance of the glass wool, and  $L_p$  is the total thickness of glass wool.

### 3.3. Metamaterial

The transfer matrix of each of the two elements of the metamaterial being known through equations 9 and 10, we can now construct the global transfer matrix of the metamaterial of Figure 1. Since these two elements are in parallel, the parallel transfer matrix method (PTMM) [22] will be used for their assembling. First, we need to define the admittance matrix of both elements by

$$Y_i = \begin{bmatrix} y_{i11} & y_{i12} \\ y_{i21} & y_{i22} \end{bmatrix} = \frac{1}{T_{i12}} \begin{bmatrix} T_{i22} & -1 \\ 1 & -T_{i11} \end{bmatrix} \quad (11)$$

where  $i = HR$  or  $GW$ , and subscripts 11, 12, 21, and 22 refer to the coefficients of transfer matrix  $i$ . Following the PTMM, the global transfer matrix of the metamaterial can be written as

$$T_G = -\frac{1}{\sum r_i y_{i21}} \begin{bmatrix} \sum r_i y_{i22} & -1 \\ \sum r_i y_{i11} - \sum r_i y_{i12} \sum r_i y_{j21} & -\sum r_i y_{i11} \end{bmatrix} \quad (12)$$

where  $r_i = S_i/S_{total}$  is the surface ratio of element  $i$  over the total surface of the metamaterial. For  $GW$ ,  $r_{GW} = (D_p^2 - t_p^2)/D_p^2$ , and for  $HR$ ,  $r_{GW} = d^2/D_p^2$ . Note that the rigid surface of the  $HR$  ( $r_{rigid} = 1 - r_{GW} - r_{HR}$ ) is also in parallel with the previous ones; however, its admittance coefficients are zero.

### 3.4. Characterization of metamaterial acoustic properties

By defining the global matrix as  $\mathbf{T}_G = [T_{G11}, T_{G12}; T_{G21}, T_{G22}]$ , the normal-incidence sound absorption coefficient (SAC) of the hard-backed metamaterial and its normal-incidence sound transmission loss (STL) are given by:

$$SAC = 1 - \left| \frac{T_{G11} - T_{G21} Z_0}{T_{G11} + T_{G21} Z_0} \right|^2 \quad (13)$$

$$STL = 20 \log_{10} \left( \frac{1}{2} \left| T_{G11} + T_{G22} + \frac{1}{Z_0} T_{G12} + Z_0 T_{G21} \right| \right). \quad (14)$$

## 4. RESULTS

Here, the developed transfer matrix method is used to predict first the normal incidence sound absorption coefficient, and second the normal incidence sound transmission loss. The design parameters of the simulated metamaterial are given in Table 2, and the JCA material parameters of the glass wool are given in Table 3. Here, the structured neck is composed of  $N = 8$  periodic unit cells.

Table 4: Design parameters in millimeters (mm) of metamaterial.

| $d$ | $\ell$ | $D$ | $h$  | $L_B$ | $L_C$ | $D_C$ | $t_p$ | $L_p$ |
|-----|--------|-----|------|-------|-------|-------|-------|-------|
| 2.5 | 2.59   | 25  | 2.83 | 44.95 | 5.05  | 40    | 9     | 52    |

Table 2: Johnson-Champoux-Allard (JCA) [23] parameters of the glass wool.

| Viscous characteristic length<br>$\Lambda$ ( $\mu\text{m}$ ) | Thermal characteristic length<br>$\Lambda'$ ( $\mu\text{m}$ ) | Tortuosity<br>( $\alpha_\infty$ ) | Static airflow resistivity<br>$\sigma$ ( $\text{Pa}\cdot\text{s}/\text{m}^2$ ) | Open porosity<br>$\Phi$ (%) |
|--|---|-----------------------------------|--|-----------------------------|
| 85   | 170   | 1                                 | 20 709   | 85                          |

For the case of sound absorption, two configurations of the metamaterial of Figure 1 are simulated. The first is the complex HR embedded in a rigid matrix, and the second is the complex HR embedded in the glass wool. For the first configuration, the same equations as described earlier are used to construct the model, except that the  $r_{GW}$  ratio is set to zero in equation 12. The results obtained with the proposed TMM and FEM calculations are compared in Figure 5. One can note that embedding the HR in the glass wool improves the sound absorption. Also, due to its structured neck, it adds multitone absorption peaks at the neck resonances compared to the case of a simple straight neck of the same length. The number of resonances is equal to the periodicity  $N$  of the structured neck. In addition, the TMM results closely correspond to the FEM calculations, thus validating the implementation of the proposed analytical method. However, there are some deviations in the position of the resonances due to the correction length, used in Equation 4, which should be improved. In addition, the sound absorption values are slightly lower than those predicted with the FEM. At the moment, we have no explanation for this difference. Note that the FEM results were obtained with the acoustic module of COMSOL Multiphysics using an axisymmetric model of the metamaterial with quartic Lagrange elements. The used model and mesh are shown in Figure 6. The convergence of the calculations was verified.

For the case of sound transmission, the TMM and FEM predictions of the sound transmission loss of the metamaterial presented in Figure 1 are shown in Figure 7. The STL of the metamaterial is also compared to a layer of glass wool of the same thickness and to the STL of the same HR with, this time, a single straight neck of the same length. There again, the comparisons between the analytical calculations proposed and the FEM calculations are close. While the classical HR with a straight neck only adds one tonal peak, the structured neck adds multitone STL peaks at its resonances. As for sound absorption, the number of resonances is equal to periodicity  $N$ . The fact that the mean STL is larger than the STL of the glass wool alone is mainly due to the fact that the equivalent airflow resistivity of the metamaterial (HR in glass wool) is larger than the resistivity of the glass wool. For the FEM simulations, an air cavity was added behind the metamaterial model shown in Figure 6 with an air impedance condition at the rear surface to simulate an anechoic termination for the STL calculation.

Note that the design parameters used in the previous simulations were not optimized with a view to improve the tonal sound absorption coefficient and the sound transmission loss at the complex HR resonances. Here, the objective of the simulations was to validate the implementation of the proposed TMM approach by comparisons with FEM calculations, and to highlight some important features of the studied metamaterial. As an interesting feature, the analytical TMM calculations only took 0.6 seconds (CPU) to solve the problem on 2951 frequency points. For the same number of frequency points, the converged FEM calculations on COMSOL Multiphysics took between 2 and 3 minutes on a personal computer equipped with an Intel® Xeon® CPU E5-1607 processor @ 3 GHz. With a view to optimize the design parameters of such a metamaterial for a given application, the proposed TMM approach is well suited.

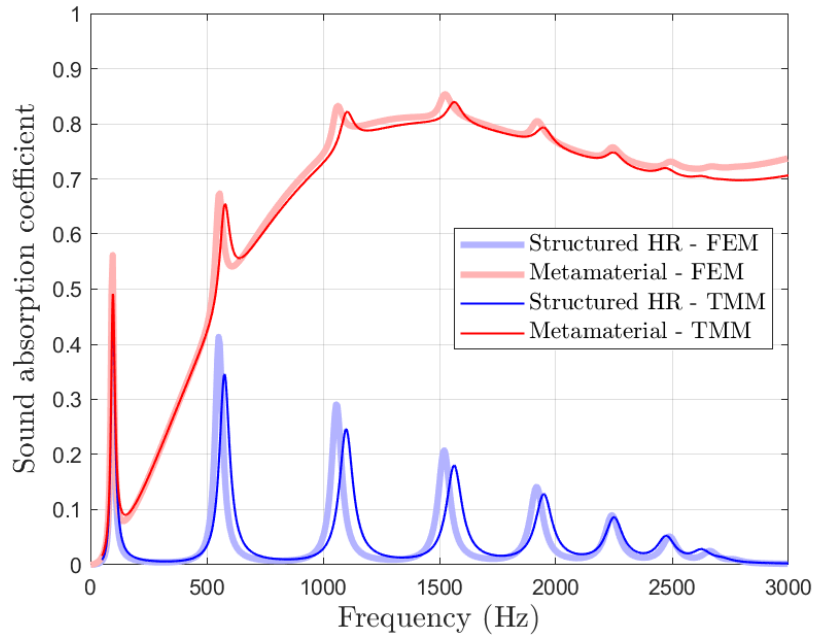


Figure 5: Sound absorption coefficient predictions using the proposed TMM model and FEM calculations on two configurations of the metamaterial.

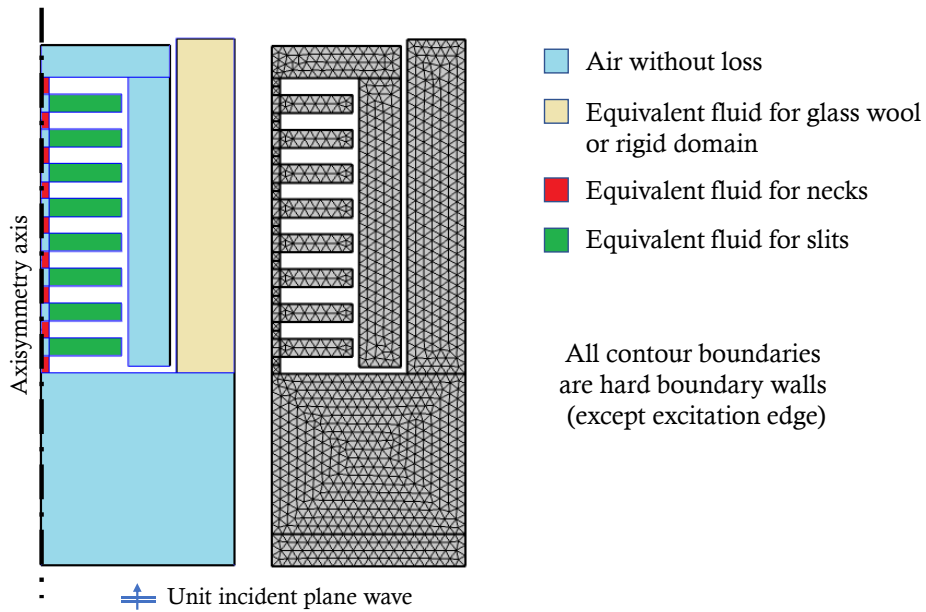


Figure 6: FEM model and mesh of the metamaterial connected to a simulated impedance tube for sound absorption calculations. The bottom rectangle represents the upstream air domain of the simulated impedance tube.

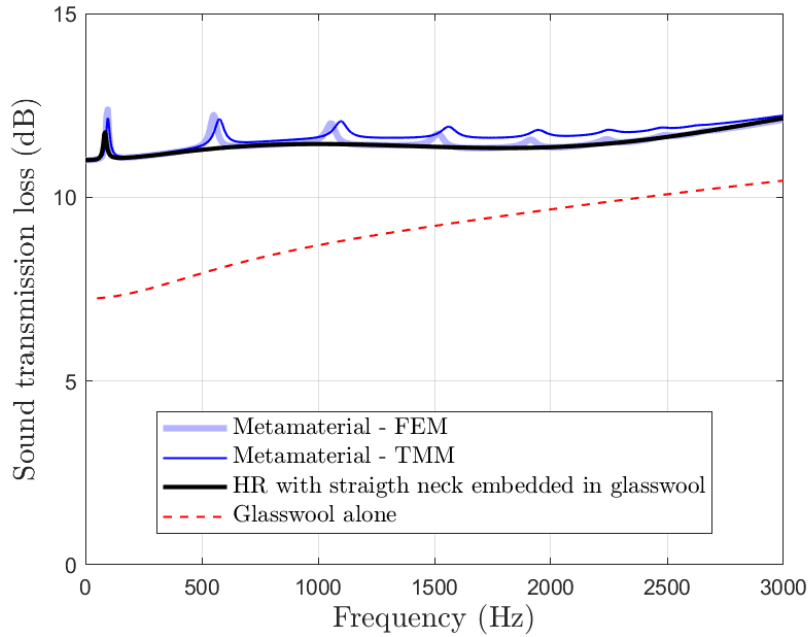


Figure 7: Sound transmission loss predictions with the proposed TMM model and FEM calculations for the proposed metamaterial.

## 5. CONCLUSIONS

This paper presented a concept of a thin acoustic metamaterial made of a complex Helmholtz resonator embedded in a porous matrix and the associated analytical transfer matrix modeling approach. The complex HR contains a structured neck which creates multitone sound absorption peaks and sound transmission loss peaks. This is an advantage compared to a conventional HR having a straight neck which only creates one tonal peak. The number of peaks of the metamaterial is equal to the periodicity  $N$  of the structured neck. The implementation of the proposed analytical modeling approach was validated by comparisons with finite element calculations. While good comparisons were obtained between the proposed approach and the FEM calculations, a slight deviation in the position of the resonances was observed. This deviation is due to the method of calculating the effective length of the neck to account for end correction. More investigation is required to improve this calculation. Also, a deviation in terms of the amplitudes was also observed. So far, the authors have no explanation for this deviation. Finally, the proposed analytical modeling requires only a fraction of the calculation time of the finite element method. Consequently, it is much suitable for optimization purpose.

While this work has shown the potential of a thin and easily integrable metamaterial in an UAS propeller shroud, capable of attenuating propeller  $N/Rev$  frequencies, several steps remain to be investigated. In particular, the optimization of the design parameters to control the resonant frequencies of the metamaterial to match the frequencies of the tonal noise.

## 6. REFERENCES

1. Oleson R & Patrick H. Small aircraft propeller noise with ducted propeller. *AIAA-98-2284, In 4th AIAA/CEAS aeroacoustics conference*, 02-04 June 1998, Toulouse, France.
2. Marte J. E & Kurtz D. W. A review of aerodynamic noise from propellers, rotors, and lift fans, *NASA CR 107568, Technical Report 32-1462*, 1970.

3. Anwar M. N. M., Vieira A., Snellen M., Dick G. S. & Veldhuis L. L. M. Experimental characterization of noise radiation from a ducted propeller of an unmanned aerial vehicle. *International Journal of Aeroacoustics*, **18**, 1-20 (2019).
4. Ohad Gur & Aviv Design of Quiet Propeller for an Electric Mini Unmanned Air Vehicle. *Journal of Propulsion and Power*, **25** (3), 717-728 (2009).
5. Pagano A., Mattia B., Damiano C. & Luigi F. Tonal and Broadband Noise Calculations for Aeroacoustic Optimization of a Pusher Propeller. *Journal of Aircraft*, **47**(3), 835-848 (2010).
6. Kone T. C. *Etude numérique de l'identification des sources acoustiques d'une pale de ventilateur* (Numerical study of the identification of the acoustic sources of a fan blade), thesis, Université de Sherbrooke, QC, Canada, 2016.
7. Seong W. C., Yu S. K. & Ji Suk L. Design and Test of Small Scale Ducted-Prop Aerial Vehicle. *AIAA 2009-1439, 47th AIAA Aerospace Sciences Meeting Including The New Horizons Forum and Aerospace Exposition*, 5 -8 January 2009, Orlando, Florida.
8. Seyit Türkmen Koç, Serdar Yılmaz, Duygu Erdem & Kavsaoğlu M. S. Experimental Investigation of a Ducted Propeller. *4<sup>th</sup> European conference for aerospace science (EUCASS)*, 4 -8 July, 2011, Saint Petersburg.
9. Gerald W. B., John W. P. & Alan S. H. Advanced turbofan duct liner concepts. *NASA-CR 1999 209002*, 1998.
10. Hughes I. J. & Dowling A. P. The Absorption of Sound by Perforated Linings. *Journal of Fluid Mechanics*, **218**, 299-335 (1990).
11. Jing X. D., Wang X. Y. & Sun X. F. Broadband acoustic liner based on the mechanism of multiple cavity resonance. *AIAA Journal*, **45**, 2429-2437 (2007).
12. Beck B. S. Grazing incidence modeling of a metamaterial-inspired dual-resonance acoustic liner. *In Proceedings of SPIE, Health Monitoring of Structural and Biological Systems 2014*, 10-13 Mars 2014, San Diego, CA, USA.
13. Beck B. S., Schiller N. H. & Jones M G. Impedance assessment of a dual-resonance acoustic liner. *Appl. Acoustics*, **93**, 15-22 (2015).
14. Auregan Y. & Leroux M. Experimental evidence of an instability over an impedance wall in a duct with ow, *International Journal of Acoustics and Vibration* **317**(3), 432-439 (2008).
15. Auregan Y., Farooqui M. & Groby J.-P. Low frequency sound attenuation in a flow duct using a thin slow sound material, *The Journal of the Acoustical Society of American*, **39** (EL149) (2016).
16. García-Chocano V. M., Graciá-Salgado R., Torrent D., Cervera F., & Sánchez-Dehesa J., Quasi-two-dimensional acoustic metamaterial with negative bulk modulus, *Physical Review*, **B85**, 184102 (2012).
17. Leclaire P., Dupont T., Panneton R. & Umnova O. Acoustical properties of air-saturated porous material with periodically distributed dead-end pores, *The Journal of the Acoustical Society of America* **137**(4), 1772-1782 (2015).
18. T. Dupont, Leclaire P., Panneton R. & Umnova O., A microstructure material design for low frequency sound absorption, *Applied Acoustics*, **136**(4), 86-93 (2018).
19. Kone T. C., Panneton R. & Dupont T. Thermo-Visco-Acoustic Metamaterials to Damp Acoustic Modes in a Complex Geometry”, *26<sup>th</sup> International Congress on Sound and Vibration*, 7-11 July 2019, Montreal, Canada.
20. Kone T. C., Panneton R., Dupont T. & Ghinet S., Thermal-visco-acoustic metamaterials to damp acoustic modes in complex shape geometries at low frequencies, submission process in *JASA* (2020).
21. Kone T. C., Ghinet, S., Dupont, T., Panneton, R., Anant, G. & Wickramasinghe V. Characterization of the acoustic properties of complex shape metamaterials. In *Proceedings of 49<sup>th</sup> International Congress on Noise Control Engineering, INTER-NOISE 2020*, 23-26 August 2020, Seoul, South Korea.
22. Verdier K., Panneton R., Elkoun S., Dupont T., and Leclaire P., Transfer matrix method applied to the parallel assembly of sound absorbing materials, *JASA*, **134**, 4648-4658 (2013).
23. Champoux Y. & Allard J., Dynamic tortuosity and bulk modulus in air-saturated porous media, *Journal of Applied Physics*, **70**(4), 1975-1979 (1991).

24. Dickey NS, Selamet A. Helmholtz resonators: one-dimensional limit for small cavity length-to-diameter ratios. *J SV* **195(3)**, 512–7 (1996).
25. Munjal, M. L., Galaitsis, A. G. & Ver, I. L. *Passive Silencers, Noise and Vibration Control Engineering* (eds I.L. Ver and L.L. Beranek), John Wiley & Sons, Inc., New York, 2006.